

OBSERVATIONS OF INFRARED EMISSION LINES AND RADIO CONTINUUM EMISSION FROM PRE-MAIN-SEQUENCE OBJECTS

NEAL J. EVANS II¹ AND RUSSELL M. LEVREULT¹

Department of Astronomy and Electrical Engineering Laboratory, The University of Texas at Austin

AND

S. BECKWITH^{1,2} AND MIKE SKRUTSKIE¹

Department of Astronomy, Cornell University

Received 1986 September 22; accepted 1987 February 26

ABSTRACT

Moderate-resolution ($\lambda/\Delta\lambda \sim 800\text{--}1000$) observations of the $\text{Br}\alpha$, $\text{Br}\gamma$, $\text{P}\gamma$, and $\text{H}_2 v = 1 \rightarrow 0S(1)$ emission lines are presented for 16 pre-main-sequence stars, most of which are low-mass ($M < 5 M_\odot$) objects. Brackett line emission was detected in nine of 16 objects. H_2 emission was confirmed in T Tauri and probably detected in MWC 1080 and L1551 IRS 5. Radio continuum observations at 6 cm are also presented. These results are compared to the predictions of existing models for stellar winds. The results are also compared to the data on molecular outflows. As has been found for higher mass stars, the mass-loss rates derived from CO would imply stronger infrared line and radio continuum emission than we observe. We discuss a number of explanations for this discrepancy and conclude that largely neutral winds provide the most attractive explanation.

Subject headings: infrared: spectra — stars: pre-main-sequence

I. INTRODUCTION

Mass loss in pre-main-sequence (hereafter PMS) stars can have a significant effect on PMS evolution, the dynamics in the surrounding molecular cloud, and the formation of planetary systems. P Cygni profiles seen in $\text{H}\alpha$ lines from T Tauri stars provided the earliest evidence of mass loss (Kuhi 1964) in these relatively low-mass PMS stars. Radio continuum and infrared emission lines from hydrogen, with properties unlike those of photoionized H II regions, were interpreted as stellar winds from somewhat more massive, embedded PMS stars (e.g., Felli *et al.* 1982). The discovery of molecular outflows, revealed by broad wings on CO spectra, has shown that the mass loss has occurred over fairly long periods ($10^3\text{--}10^5$ yrs) and extends from very high mass objects (e.g., Bally and Lada 1983) to fairly low mass PMS stars (e.g., Levreault 1985). There are many theoretical models for producing the mass loss (e.g., Königl 1982; Hartmann, Edwards, and Avrett 1982; Pudritz and Norman 1983, 1986; Uchida and Shibata 1985; Draine 1983; Phillips and Beckman 1980; Torbett 1984) but no consensus has been reached on the relative merits of these different models.

One reason that it has been hard to test the different models is that quantitative measurements of the mass-loss rates have been difficult to obtain. The molecular outflows have provided a means for measuring the mass-loss rates averaged over the duration of the phenomenon for a large number of objects (e.g., Bally and Lada 1983; Levreault 1985; Lada 1985). Unfortunately, the mass-loss rates derived from the molecular data are usually higher (sometimes by orders of magnitude) than those derived from other means (see, e.g., Snell and Bally 1986). In order to study this problem, we have observed infrared hydrogen lines and radio continuum emission from a sample of

PMS stars which have been observed in the $J = 2 \rightarrow 1$ CO line to search for molecular outflows (Levreault 1985); the PMS stars in this sample have masses in the range of 1–10 M_\odot , with most near 2–3 M_\odot , and spectral types ranging from M to B. Thus, in general, we are extending the study of molecular outflows to lower mass PMS stars than were studied by Bally and Lada (1983). This paper in particular extends to lower mass stars the study of infrared line and radio continuum emission. We observed $\text{Br}\alpha$, $\text{Br}\gamma$, and $\text{P}\gamma$ lines and obtained radio measurements at a wavelength of 6 cm within 1 month of one set of the line measurements. Finally, we searched for H_2 emission in the $v = 1 \rightarrow 0 S(1)$ line as an indicator of shocks in molecular material near the stars.

II. OBSERVATIONS

a) Infrared

The infrared observations were made during 1983 November 25–28 and 1985 January 4–7 at the Infrared Telescope Facility³ (IRTF) with the cooled grating spectrometer described by Beckwith *et al.* (1983). Modulation of the secondary with a 20" (north-south) throw at 5 Hz provided sky cancellation, and standard demodulation and data collection techniques were used to record spectra digitally. The spatial resolution was set by the entrance diaphragm at 6" in 1983; resolutions of both 3".5 and 5".3 were used in 1985. The spectral resolution was set by the exit aperture and the order sorting filters; the resolving power ($\lambda/\Delta\lambda$) was roughly 800 in 1983 and 1000 in 1985 (see Table 1).

Observations of the emission lines from NGC 7027 (in 1983) and T Tau (in 1985) gave a precise determination of the wavelength scale for the same lines in the other sources. Observations of IRTF standard stars, listed in Table 2, set the flux density scale to about 10%, based on a comparison of the different standards. For absolute calibration, we assumed that

¹ Visiting Astronomer at the Infrared Telescope Facility, which is operated by the University of Hawaii under contract from the National Aeronautics and Space Administration.

² Alfred P. Sloan Fellow.

³ The Infrared Telescope Facility is operated by the University of Hawaii under a contract from NASA.

TABLE 1

INSTRUMENTAL RESOLVING POWER

| Line | λ (μm) | 1983 $\lambda/\Delta\lambda$ | 1985 $\lambda/\Delta\lambda$ |
|----------------------|--------------------------------|---------------------------------|---------------------------------|
| H ₂ | 2.1202 | 825 | 1100 |
| Br γ | 2.1644 | 860 | 1140 |
| Pf γ | 3.7416 | ... | 900 |
| Br α | 4.0504 | 770 | 1020 |

Vega has flux densities of 646 Jy at *K* (2.2 μm) and 278 Jy at *L* (3.5 μm) (Neugebauer, private communication; Campins, Rieke, and Lebofsky 1985), and we extrapolated these values to find the magnitudes of the standard at the wavelengths of the spectral lines by assuming the stellar intensities follow a Planck function at a temperature characteristic of their spectral types. Because most of the standard stars show H I lines in absorption, only the baseline outside the absorption was used to set the continuum level.

The observing strategy began with observations of Br γ and H₂ for each star in our sample. If Br γ was detected, observations were also made of Br α , and in some cases, Pf γ was also observed.

b) Radio Continuum

The radio continuum observations were made on 1984 December 13 at a wavelength of 6 cm using the A-configuration of the NRAO⁴ Very Large Array. The flux calibrator 3C48 was observed at the end of the run, and we assumed that its 6 cm flux density is 5.36 Jy. Recently 3C 48 has varied, but only by $\sim 5\%$. By using 10 different phase calibrators, it was possible to have a phase calibrator near each source. Use of natural weighting and no taper for the final maps maximized the sensitivity to weak sources and produced a beam of $\sim 0''.5$. The RMS noise was typically 50–160 μJy .

III. RESULTS

Table 3 presents the infrared continuum flux densities and emission-line fluxes for the stars in the sample, along with the radio continuum flux densities. Fits of the instrumental wavelength response to the data, as shown in Figure 1, gave both the line fluxes and uncertainties. None of the lines showed evidence of being resolved; we can set a limit to the intrinsic line widths of $\sim 200 \text{ km s}^{-1}$ for the stronger emission lines.

⁴ The NRAO is operated by Associated Universities, Inc., under contract to the National Science Foundation.

TABLE 2
STANDARD STARS

| STAR | Mag | | H ₂ <i>S_v</i> (2.12 μm) (Jy) | Br γ <i>S_v</i> (2.17 μm) (Jy) | Pf γ <i>S_v</i> (3.74 μm) (Jy) | Br α <i>S_v</i> (4.05 μm) (Jy) | Sp. Type | <i>T</i> _* |
|---------------|--|--|--|---|---|---|----------|-----------------------|
| | <i>K</i> (2.2) (<i>S_v</i> [Jy]) | <i>L</i> (3.5) (<i>S_v</i> [Jy]) | | | | | | |
| 1983 Data | | | | | | | | |
| BS 8551 | 2.30 (77) | 2.24 (35) | 80 | 78 | | 28 | K0 III | 4400 |
| BS 0531 | 3.89 (18.0) | 3.94 (7.38) | 19 | 18 | | 5.8 | F2 IV | 7000 |
| BS 0718 | 4.37 (11.5) | 4.44 (4.66) | 12.2 | 11.8 | | 3.57 | B9 III | 12,000 |
| BS 1412 | 2.92 (44) | ... | 47 | 45 | | <u>15.8^a</u> | A7 III | 8500 |
| BS 1763 | 6.28 (1.99) | 6.30 (0.840) | 2.13 | 2.05 | | 0.64 | B1 V | 21,500 |
| BS 3975 | 3.43 (27.4) | ... | 29.0 | 28.1 | | <u>9.81^a</u> | A0 I | 8500 |
| BS 4133 | 4.32 (12.1) | 4.08 (6.49) | 13.0 | 12.5 | | 4.9 | B1 I | 25,000 |
| 1985 Data | | | | | | | | |
| BS 2491 | -1.32 (2180) | ... | 2315 | 2230 | <u>875^a</u> | <u>758^a</u> | A1 V | 9900 |
| BS 2943 | -0.65 (1180) | -0.66 (510) | 1243 | 1203 | 445 | 400 | F5 IV | 6580 |
| BS 1412 | 2.92 (44) | ... | 47 | 45 | <u>18^a</u> | <u>16^a</u> | A7 III | 8500 |
| BS 8541 | 4.24 (13) | 4.23 (5.7) | 14 | 13 | 5.1 | 4.4 | B9 I | 13,000 |
| BS 0337 | -1.87 (3615) | -2.01 (1770) | 3700 | 3615 | 1630 | 1470 | M0 III | 3200 |
| BS 8775 | -2.22 (4990) | -2.39 (2510) | 5085 | 5031 | 2320 | 2100 | M2 II | 3000 |
| BS 5191 | 2.37 (73) | 2.35 (32) | 78 | 75 | 28 | 24 | B3 V | 18,000 |
| BS 4133 | 4.32 (12.1) | 4.08 (6.49) | 12.9 | 12.5 | | | B1 I | 25,000 |
| BS 3975 | 3.43 (27.4) | ... | 28.6 | 28.0 | | | A0 I | 8500 |

^a Underlined quantities indicate that no *L* magnitude is available for the star and the *K* magnitude has been used.

1987ApJ...320...364E

TABLE 3
OBSERVATIONAL RESULTS

| No. | Source | Date | S_ν (2.16 μm) (Jy) | S_ν (4.05 μm) (Jy) | F_ν (H_2) ($10^{-16} \text{ W m}^{-2}$) | F_ν (Br γ) ($10^{-16} \text{ W m}^{-2}$) | F_ν (Pfy) ($10^{-16} \text{ W m}^{-2}$) | F_ν (Br α) ($10^{-16} \text{ W m}^{-2}$) | Peak S_ν (6 cm) (mJy) | Total S_ν (6 cm) (mJy) |
|---------|-------------------|------|---------------------------------------|---------------------------------------|---|---|--|---|---------------------------------|----------------------------------|
| 1..... | Lk H α 198 | 1985 | 1.4 \pm 0.1 | 4.5 \pm 0.5 | <5 | 4.4 \pm 0.6 | <4 | 6.6 \pm 1.0 | <0.44 | ... |
| 2..... | RNO 13 | 1985 | 0.08 \pm 0.03 | ... | <4 | <4 | ... | ... | <0.18 | ... |
| 3..... | RNO 15 | 1985 | 0.31 \pm 0.04 | ... | <4 | <4 | ... | ... | <0.32 | ... |
| 4..... | RY Tauri | 1985 | 3.6 \pm 0.5 | ... | <6 | <5 | ... | ... | <0.27 | ... |
| 5..... | T Tauri | 1983 | 4.1 \pm 0.4 | 5.9 \pm 0.6 | 6.9 \pm 0.7 | 4.4 \pm 0.4 | ... | 15. \pm 1.5 | ... | ... |
| 6..... | DG Tauri | 1985 | 4.5 \pm 0.4 | 7.0 \pm 0.7 | 5.3 \pm 0.4 | 6.0 \pm 0.5 | 3.4 \pm 0.5 | 12. \pm 1.4 | 3.2 \pm 0.1 | 6.4 |
| 7..... | L1551 IRS 5 | 1985 | 1.0 \pm 0.1 | 2.8 \pm 0.2 | <1.7 | 6.8 \pm 0.7 | ... | 5.5 \pm 1.0 | ... | 0.6 |
| 8..... | HL Tauri | 1983 | 1.1 \pm 0.1 | 2.8 \pm 0.3 | <5 | 6.9 \pm 0.9 | ... | 5.7 \pm 0.9 | 0.5 \pm 0.05 | ... |
| 9..... | XZ Tauri | 1985 | 0.1 \pm 0.01 | ... | 0.7 \pm 0.2: | <5 | ... | ... | 1.4 \pm 0.07 | 5.0 |
| 10..... | AB Aurigae | 1985 | ... | ... | ... | ... | ... | ... | ... | ... |
| 11..... | C-S Star | 1983 | 0.84 \pm 0.08 | 3.1 \pm 0.3 | <1.7 | 2.7 \pm 0.3 | ... | 7.9 \pm 0.8 | ... | ... |
| 12..... | V380 Orionis | 1985 | 0.63 \pm 0.06 | 2.8 \pm 0.3 | <4 | 1.5 \pm 0.4: | <4 | 4.2 \pm 1.0 | <0.17 ^a | ... |
| 13..... | FU Orionis | 1985 | 0.60 \pm 0.06 | 1.3 \pm 0.1 | ... | 2.1 \pm 0.5 | ... | 2.5 \pm 0.5 | ... | ... |
| 14..... | R Mon | 1985 | 0.58 \pm 0.06 | ... | <4 | <4 | ... | ... | <0.17 ^a | ... |
| 15..... | Z CMa | 1983 | 14. \pm 1.4 | 17. \pm 1.7 | <8 | 32. \pm 3. | 11. \pm 1.3 | 33. \pm 3. | <0.16 | ... |
| 16..... | MWC 1080 | 1985 | <0.15 | ... | <4 | <6 | ... | ... | <0.17 | ... |
| 17..... | | 1985 | 2.5 \pm 0.2 | 4.2 \pm 0.4 | <1.7 | 13. \pm 2. | ... | 13. \pm 1.3 | ... | ... |
| 18..... | | 1985 | 2.0 \pm 0.2 | 4.0 \pm 0.4 | <4 | 10. \pm 1.2 | 5.6 \pm 0.7 | 12. \pm 1.4 | <0.17 | ... |
| 19..... | | 1985 | 6.0 \pm 0.6 | ... | <13 | <6 | ... | ... | <0.17 | ... |
| 20..... | | 1985 | 2.6 \pm 0.2 | ... | <5 | <3 | ... | ... | <0.17 | ... |
| 21..... | | 1985 | 2.7 \pm 0.3 | ... | <8 | ... | ... | <20 | ... | ... |
| 22..... | | 1983 | 24. \pm 2. | 44. \pm 4. | <34 | 29. \pm 6. | ... | ... | ... | ... |
| 23..... | | 1985 | 22. \pm 2. | 65. \pm 7. | <13 | 19. \pm 5. | <18 | 31. \pm 5. | 0.7 \pm 0.06 | 2.0 |
| 24..... | | 1985 | 6.6 \pm 0.7 | 16. \pm 1.6 | 2.2 \pm 0.5: | 26. \pm 4. | 11. \pm 1.3 | 26. \pm 3. | <0.43 | ... |

^a Detected in C-array at 0.25 mJy (Brown, Mundt, and Drake 1985).

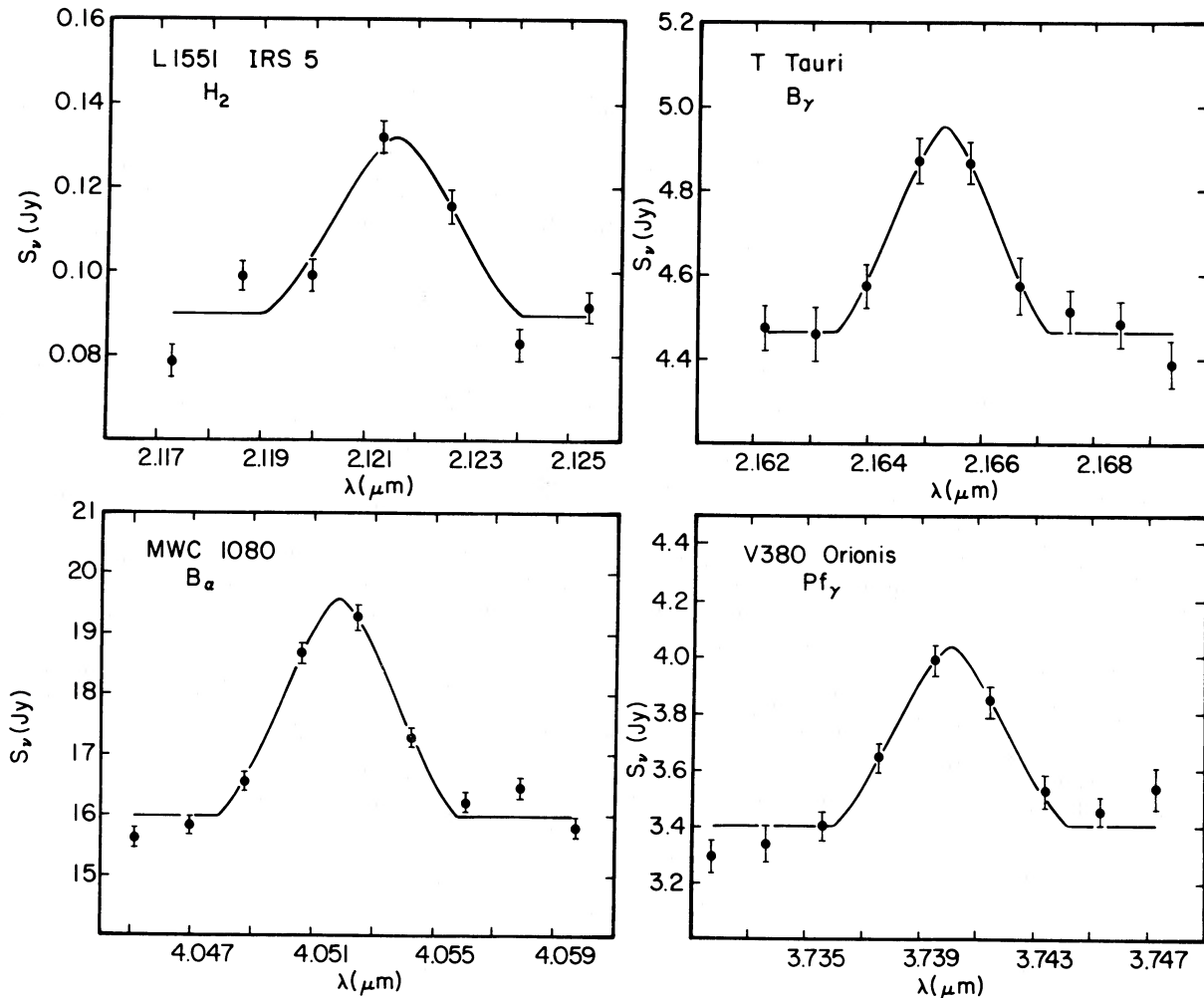


FIG. 1.—Four spectra are shown with the best-fitting instrumental profile drawn as a solid line. The H_2 line in L1551 is an example of what we consider a marginal detection, while the other lines all have higher signal-to-noise ratio.

Entries in the table which are followed by a colon are marginal detections, of the order $3-5\sigma$, which should be confirmed. The uncertainties in the table are the 1σ uncertainties from the fit of the instrumental profile to the line, with a $\pm 10\%$ calibration error added in quadrature. Upper limits to line fluxes are visual estimates of the weakest line which can be convincingly ruled out; this usually corresponds to a 3σ upper limit, but may be larger when the baselines are uncertain. The uncertainties are clearly larger for sources with strong continua, since in these cases the seeing, scintillation, and tracking errors increase the absolute uncertainties. The upper limits to radio continuum flux densities are 3σ where σ is the rms noise in the map; for detections, the uncertainties are the rms noise in the maps.

Among the 16 objects observed, nine show detectable H I line emission, including three where it was previously known. H_2 lines are confirmed in T Tauri (Beckwith *et al.* 1978; Brown *et al.* 1981, Zinnecker *et al.* 1985) and marginally detected in L1551 IRS 5 (see Fig. 1) and MWC 1080.

PMS stars are known to vary optically, both in line and continuum emission. Our data indicate that the infrared continua and H I lines may also vary. We have examined this issue on the basis of measurement on consecutive nights of T Tauri, and in both observing sessions (1983 and 1985) for six stars with detected H I line emission. T Tau was observed on three

of the four nights in 1985 with no significant differences, but the H_2 and Br_γ lines varied (in opposite directions) by about 30% between 1983 and 1985, while the continuum level remained nearly constant. After a 30% correction for a different calibration, the original detection of these lines (Beckwith *et al.* 1978) indicates little variation in the H_2 line and a Br_γ line flux of $11 \times 10^{-16} \text{ W m}^{-2}$, about twice the strength of the present observations, but the original Br_γ line strength may have been overestimated because of Br_γ absorption in the standard star (β Per). The Br_α line flux from T Tau has not changed significantly between 1983 and 1985, and the 1982 December equivalent width of Persson *et al.* (1984), combined with our continuum measurements, leads to a Br_α line flux in good agreement with our measurements. There is marginal evidence for Br_γ variation in Z CMa between the 1983 and 1985 observations. The strongest evidence for substantial line flux variations exists for HL Tau. In addition to the variations apparent in Table 2, comparison to measurements by Persson *et al.* (1984), Thompson (1987), and M. Simon (private communication) indicate variations in both Br_α and Br_γ by factors greater than 2 on time scales of years.

This examination of the line flux data leads us to several conclusions. There is fairly strong evidence for variation in the line fluxes on time scales of years, but not on time scales of

days. The variations are not obviously correlated with variations in the adjacent continuum levels which, however, also vary. This result probably explains many of the discrepancies among data obtained by different observers that were noted by Persson *et al.* In particular, continuum variations make determination of line fluxes from equivalent widths uncertain. Furthermore, the beam sizes should be the same, since there is some evidence for extended H₂ emission in T Tau (Beckwith *et al.* 1978).

Four of the 16 sources in Table 3 were detected at 5 GHz. Since the radio observations were made only 25 days before the 1985 infrared observations, we list them on the same line as the 1985 infrared measurements, but the reader should note they are not truly simultaneous. Comparison of our peak flux densities with previous data taken with similar resolution (Cohen, Bieging, and Schwartz 1982; Bieging, Cohen, and Schwartz 1984) indicates excellent agreement. All of our detected sources were resolved to some extent and the maps are in good agreement with previous maps, except at the lowest contour levels. The maps were CLEANed to determine the total flux densities given in Table 3. The total flux densities are sensitive to the lowest level emission; thus there are greater differences among the various total flux density measurements (ours; Cohen, Bieging, and Schwartz; Bieging, Cohen, and Schwartz), but these differences are still, at worst, a factor of 2. In the cases of HL Tau and XZ Tau, our upper limits (<0.17 mJy) are lower than detections by Brown, Mundt, and Drake (1985), who detected emission from each of these two stars with peak flux densities of 0.25 mJy in C-array. The emission around HL Tau was extended, and additional extended emission was seen in the vicinity of these sources. It is likely that our A-array observations would resolve out the 6 cm extended emission seen by Brown, Mundt, and Drake (1985),

and some decrease in flux is already seen with B-array observations (0.22 mJy for HL Tau; 0.14 mJy for XZ Tau—Brown, Drake, and Mundt 1986).

IV. DISCUSSION

a) The Origin of the Infrared Line and Radio Continuum Emission

One of the problems encountered by earlier studies of infrared line and radio continuum emission from more massive and deeply embedded pre-main-sequence stars was that the very poorly known extinction could have a substantial effect on the line fluxes and ratios. For example, Simon *et al.* (1983) had to infer the extinction to most objects by comparing observed line ratios to the values predicted by their models. To test the models, it is preferable to study objects with known extinction. Because estimates of visual extinction are available for the stars in our study, the line fluxes can be corrected for interstellar extinction. The extinction at the wavelengths of the H I lines was computed from A_v (see Table 4) and two reddening laws, a van de Hulst No. 15 law (as extended into the infrared by Becklin *et al.* [1978] and Landini *et al.* [1984]) and the law advocated by Rieke and Lebofsky (1985). Because the A_v to these objects is small and the extinction in the infrared is much less ($A_{4\mu m} \approx 0.038A_v$), the corrections are small and the differences between the two extinction laws were never significant compared to other sources of uncertainty. The extinction-corrected line fluxes (F_l^*) in Table 4 are the averages of those obtained with the two different extinction laws.

The first question we address with these data is what kind of region produces the infrared H I lines and the radio continuum emission. For optically thin H II regions, there is a linear relation between radio continuum flux density and Br α line flux.

TABLE 4
LINE FLUXES AND RATIOS CORRECTED FOR EXTINCTION^a

| No. | Source | A_v (mag) | Ref | F_l^* (Br γ) (10^{-16} W m $^{-2}$) | F_l^* (Pfy) (10^{-16} W m $^{-2}$) | F_l^* (Br α) (10^{-16} W m $^{-2}$) | Br α /Br γ | Br α /Pfy | Date |
|---------|-------------------|----------------|-----|--|---|--|--------------------------|------------------|------|
| 1..... | Lk H α 198 | 4.5 | 1 | 6.7 \pm 1.0 | <5 | 7.80 \pm 1.2 | 1.2 \pm 0.2 | >1.6 | 1985 |
| 2..... | RNO 13 | 2.7 | 2 | <5 | ... | ... | ... | ... | 1985 |
| 3..... | RNO 15 | ... | ... | ... | ... | ... | ... | ... | 1985 |
| 4..... | RY Tau | 1.9 | 1 | <6 | ... | ... | ... | ... | 1985 |
| 5..... | T Tau | 1.4 | 1 | 5.0 \pm 0.5 | ... | 15.6 \pm 1.6 | 3.1 \pm 0.4 | ... | 1983 |
| | | 1.4 | 1 | 6.8 \pm 0.7 | 3.6 \pm 0.5 | 12.5 \pm 1.4 | 1.8 \pm 0.3 | 3.5 \pm 0.6 | 1985 |
| 6..... | DG Tau | 2.4: | 3 | 8.5 \pm 0.9 | ... | 6.1 \pm 1.5 | 0.7 \pm 0.2 | ... | 1983 |
| | | 2.4: | 3 | 8.6 \pm 1.1 | ... | 6.2 \pm 1.0 | 0.7 \pm 0.14 | ... | 1985 |
| 7..... | L1551 IRS 5 | 19 \pm 2 | 4 | <35 | ... | ... | ... | ... | 1983 |
| 8..... | HL Tau | 7: | 5 | 5.4 \pm 0.7 | ... | 10.0 \pm 1.0 | 1.9 \pm 0.3 | ... | 1983 |
| | | 7: | 5 | 2.9 \pm 0.8 | <6 | 5.5 \pm 1.3 | 1.9 \pm 0.7 | >0.9 | 1985 |
| 9..... | XZ Tau | 3: | 1 | 2.9 \pm 0.7 | ... | 2.8 \pm 0.6 | 1.0 \pm 0.3 | ... | 1983 |
| | | 3: | 1 | <5 | ... | ... | ... | ... | 1985 |
| 10..... | AB Aur | 0.65 | 1 | 34. \pm 3. | 11. \pm 1.3 | 34. \pm 3. | 1.0 \pm 0.14 | 3.1 \pm 0.5 | 1985 |
| 11..... | C-S Star | 5.7 | 6 | <11 | ... | ... | ... | ... | 1985 |
| 12..... | V380 Ori | 1.5 | 7 | 15. \pm 1.5 | ... | 14.0 \pm 1.4 | 0.9 \pm 0.13 | ... | 1983 |
| | | 1.5 | 7 | 11. \pm 1.4 | 6.0 \pm 0.8 | 13.0 \pm 1.5 | 1.2 \pm 0.20 | 2.2 \pm 0.4 | 1985 |
| 13..... | FU Ori | 2.5 | 1 | <8 | ... | ... | ... | ... | 1985 |
| 14..... | R Mon | 4.2 | 1 | <5 | ... | ... | ... | ... | 1983 |
| | | 4.2 | 1 | <11 | ... | ... | ... | ... | 1985 |
| 15..... | Z CMa | 2.8: | 1 | 38. \pm 8. | ... | <22 | <0.6 | ... | 1983 |
| | | 2.8: | 1 | 15. \pm 7. | <21 | 34. \pm 6. | 1.4 \pm 0.5 | >1.6 | 1985 |
| 16..... | MWC 1080 | 5.4 | 1 | 43. \pm 7. | 14. \pm 1.7 | 32. \pm 4. | 0.7 \pm 0.1 | 2.3 \pm 0.4 | 1985 |

^a Values are averages of results from using two different extinction laws (van de Hulst No. 15 and Rieke and Lebofsky); the differences are never significant compared to other uncertainties.

REFERENCES.—(1) Cohen and Kuhi 1979; (2) Levreault 1985; (3) Kuhi 1974; (4) Snell *et al.* 1985; (5) Cohen 1983; (6) Cohen and Schwartz 1979; (7) Finkenzeller and Mundt 1984.

This relation is indicated by the dashed line in Figure 2. None of the observations is consistent with this relation, the radio emission being far too weak for a given Br α line flux. Further evidence is provided by the ratios of infrared lines (see Table 4). For optically thin emission, the line ratios are given by

$$\frac{\text{Br}\alpha}{\text{Br}\gamma} = 2.421 \frac{b_5}{b_7} e^{3090/T};$$

$$\frac{\text{Br}\alpha}{\text{P}\gamma} = 7.013 \frac{b_5}{b_8} e^{3850/T},$$

where b_n is the departure coefficient of level n from LTE (cf. Spitzer 1978). The resulting ratios are plotted in Figure 3 for a range of temperatures. It is clear that optically thin line emission, with either LTE or Menzel Case B values for the b_n 's, is inconsistent with the data. The data in Figures 2 and 3 show that the Br α line is optically thick and that the radio emission does not originate in static, photoionized, optically thin H II

regions. These conclusions agree with those reached for more luminous objects by Simon *et al.* (1983) and McGregor, Persson, and Cohen (1984).

For optically thick winds, the emission will depend on the geometry of the wind and on its temperature, density, and velocity structure. Simon *et al.* (1983) have computed the emission expected from a simple model of spherical, isothermal, fully ionized winds which begin at an inner radius r_i and recombine at an outer radius r_o ; the populations of the hydrogen energy levels are assumed to be in LTE. Since the stars we are studying are generally cooler and less luminous than those considered by Simon *et al.* (1983), it is likely that some of their assumptions are no longer appropriate, but the models are still useful as a guide in interpreting the observations.

The models show that, as the mass-loss rates increase, the line ratios (Br α /Br γ and Br α /P γ) decrease from their optically thin values (the dash-dot line in Fig. 3) and reach minimum values which depend on the effective radiating surface areas times the Planck functions for each line. The lowest line ratios

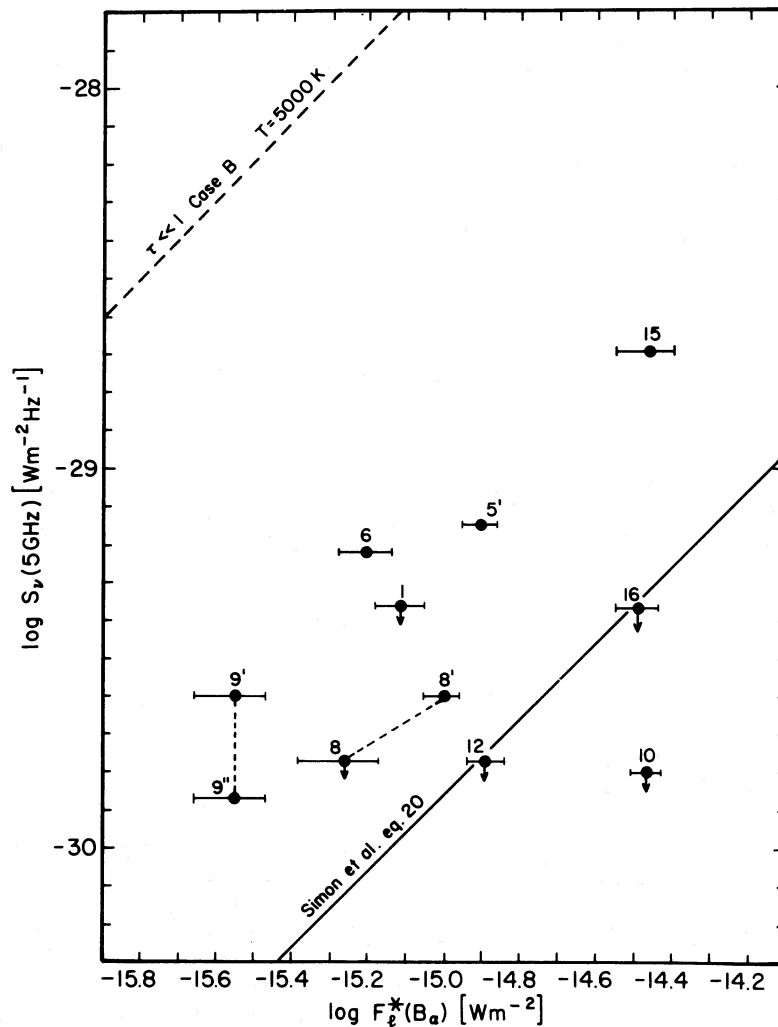


FIG. 2.—The total radio continuum flux densities are plotted vs. the Br α line fluxes. The numbers refer to the source number given in the tables. The dashed line is the relation expected for an optically thin H II region with Case B recombination at 5000 K; higher temperatures will predict more radio emission. The solid line is equation (20) of Simon *et al.* (1983). The arrows indicate 3σ upper limits. The points marked 8' and 9' combine our 1983 November infrared data with the 1984 May C-array data of Brown, Mundt, and Drake (1985); the point marked 9'' is 1985 B-array data (Brown, Drake, and Mundt 1986) and our 1983 infrared data. The point marked 5' combines our 1985 F_i^* (Br α) with the radio data for T Tau (N) of Schwartz, Simon, and Campbell (1986).

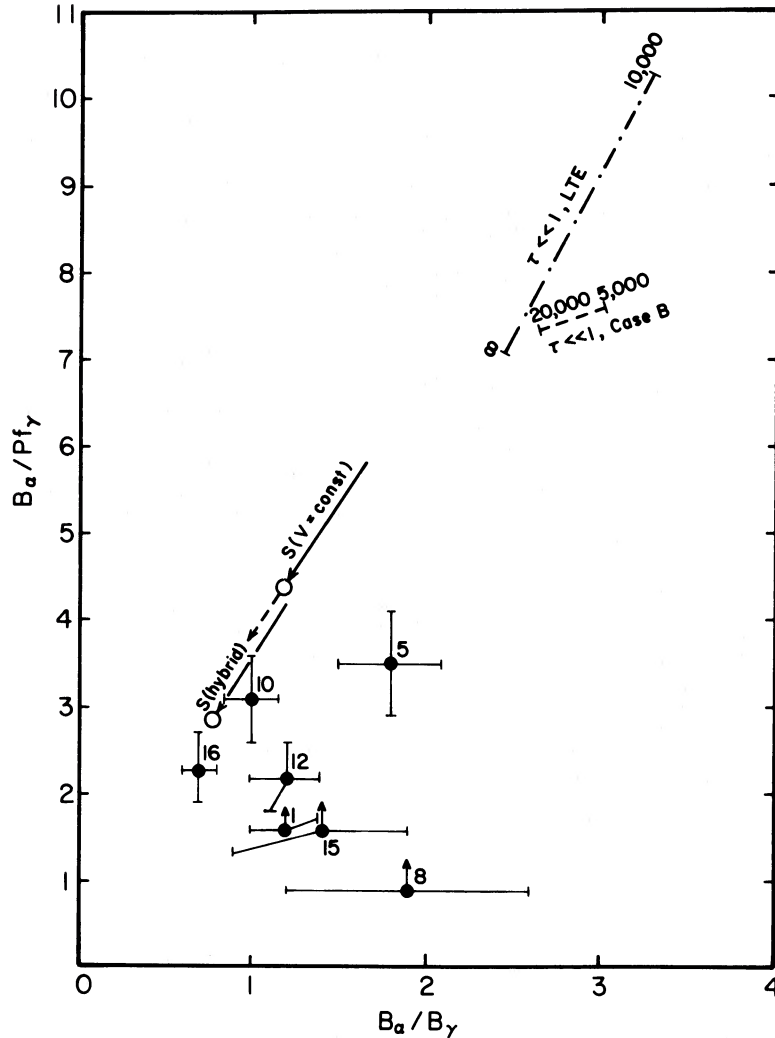


FIG. 3.—The ratios of line fluxes are plotted with error bars. The numbers refer to the source numbers in the tables. Ratios expected for optically thin emission from a gas in LTE and obeying Menzel Case B recombination are shown by the dash-dotted and dashed lines, where the numbers refer to the assumed temperature. The circles in the lower left are the minimum ratios predicted by the models of Simon *et al.* (1983) for the constant outflow velocity and the “hybrid” model ($v \propto r$), respectively, while the arrows indicate how the ratios change as the mass-loss rates increase. The dashed arrow leaving the circle for the constant velocity model shows the effect of decreasing r_o/r_i .

produced by the constant velocity models are indicated by the upper circle in Figure 3; while the thick models are clearly closer to our data than are the optically thin models, the observed $Br\alpha/Pf\gamma$ ratios are clearly lower than this minimum value. The lower circle in Figure 3 is the minimum value reached by a hybrid model with velocity proportional to radius for small radii and constant for large radii; this model can explain all but two of the lowest $Br\alpha/Pf\gamma$ ratios. Alternatively, models in which the wind recombines at small radii ($r_o/r_i \lesssim 100$ in Fig. 1 of Simon *et al.* 1983) result in smaller $Br\alpha/B\gamma$ and $Br\alpha/Pf\gamma$ ratios because the $Br\alpha$ emission is produced at considerably larger radii than are the other two lines; decreasing r_o in the constant velocity model will move the line ratios in the direction of the dashed arrow in Figure 3. Thus, the simplest models of Simon *et al.*, or plausible variations in them, can explain the observed $Br\alpha/Pf\gamma$ ratios.

A feature of the line ratios which is not well-explained is the relatively large values of $Br\alpha/B\gamma$ observed in several sources. For those sources with only upper limits on $Pf\gamma$, the models could in principle reproduce the $Br\alpha/B\gamma$ line ratios with lines

of low optical depth, but this explanation only works for quite low mass-loss rates. Detection of $Pf\gamma$ lines for these sources can test this explanation. For the two sources where we already have $Pf\gamma$ detections (T Tau and V380 Ori—points 5 and 12), no simple explanation presents itself, because most effects which raise $Br\alpha/B\gamma$ will also raise $Br\alpha/Pf\gamma$, so that the predicted line ratios move along the arrows in Figure 3. Put another way, the $Br\gamma/Pf\gamma$ ratio is lower (~ 1.9) than the ratio (~ 3.4) predicted by the models. This ratio is insensitive to r_o/r_i or, more generally, the geometry because the two lines have similar optical depths and hence should form at similar radii.

Several recent generalizations or improvements on Simon *et al.*'s models may be relevant. Smith *et al.* (1987) have developed approximate analytic expressions for the line ratios for power-law velocity fields with arbitrary exponents. These expressions indicate that negative exponents (decelerating flows) do not fit our data very well; exponents between 0 and 1 (constant velocity or $V \propto r$) give line ratios which are closer to the observed values. Chalabaev (1986) has used the Sobolev approximation to compute the source function, but a more accurate method

(Bertout 1984) to compute the emergent line profile. For the same parameters as the hybrid model of Simon *et al.*, he finds that the Br γ line is narrower than Br α , and has more P Cygni absorption, resulting in a Br α /Br γ ratio of ~ 2.0 rather than 0.8, for high mass-loss rates. He did not consider P γ lines. Höflich and Wehrse (1987) have developed non-LTE models for stellar winds and find lower Br γ /P γ ratios (~ 2.2) for some parameters. These results suggest that accurate determination of line ratios in objects with low extinction will prove useful in testing the more elaborate models which are now being considered.

We can also compare the observations to the model predictions of the radio continuum emission, though with greater uncertainty, both observational and theoretical. We have plotted our total radio flux densities in Figure 2, and we have added radio data from other observers, as identified in the figure caption. For HL Tau and XZ Tau (sources 8 and 9), the effects of differing spatial resolution are apparent. For source 5 (T Tauri), we have not plotted our radio data because we measure only T Tau (S), the infrared companion. The similarity of the Br α and H α profiles (Persson *et al.* 1984) and the high extinction to the infrared companion (R. Howell, private communication) both suggest that the infrared lines come from the optically visible star. The point (5') plotted in Figure 2 combines our Br α line flux with the radio flux density from the optically visible star (Schwartz, Simon, and Campbell 1986).

If the wind remains ionized to sufficiently large radii ($r_o/r_i > 10^3\text{--}10^5$), the radio continuum emission is dominated by the outer, optically thin, part of the wind (Panagia and Felli 1975). The radio emission can then be simply related to the Br α line flux. The solid line in Figure 2 is equation (20) of Simon *et al.* (1983), which applies to constant velocity outflows with $\tau(\text{Br}\alpha) \gg 1$. AB Aurigae (No. 10) which has less radio emission than predicted can be explained with the hybrid models (see Fig. 4 of Simon *et al.* 1983), or if the wind recombines at relatively smaller r_o .

The sources with more radio emission than predicted by equation (20) perhaps could be explained within the context of Simon *et al.*'s models by raising the temperature, but there is another problem. The angular diameter of the radio emission from a spherical wind is proportional to the square root of the flux density (Snell and Bally 1986); for the flux densities that we observe, all the sources should then be unresolved. Since all the sources are actually resolved, one suspects a geometrical effect. Appenzeller, Jankovics, and Ostreicher (1984) have argued for nonspherical winds in T Tauri stars, including some in our sample. While Schmid-Burgk (1982) has demonstrated that modest deviations from sphericity have little effect on the radio emission, Reynolds (1986) has shown that the more extreme case of well-collimated jets are much more efficient at producing radio flux than are spherical winds. Hamann and Simon (1986) have modeled the emission from biconical winds and find that the line emission is also enhanced, though somewhat less than the radio emission. Rather extreme geometrical assumptions (very confined cones almost face-on to the observer) would be required to explain most of the data in Figure 2.

Another possible explanation is that the radio continuum emission is produced by a totally different mechanism. Variable (Feigelson and Montmerle 1985) and non thermal (e.g., Becker and White 1985) radio emission from pre-main-sequence stars suggest that flare phenomena may be important. The very extended emission seen around HL and XZ Tau

by Brown, Mundt, and Drake (1985) could be due to reionization when the stellar wind is shocked as it impinges on dense parts of the surrounding cloud. Similar mechanisms could apply closer to the stars as the wind strikes a circumstellar disk (see, e.g., Rodriguez *et al.* 1986). In these cases, the radio continuum emission would not be simply related to the mass-loss rate.

We conclude that the infrared line emission is likely to be produced in stellar winds of the general type suggested by Simon *et al.* (1983), though generalizations of those models will apparently be needed to explain some aspects of the line ratios. The radio continuum emission is more problematical; it is unlikely to be a reliable indicator of the mass-loss rate for these objects.

b) Comparison to the CO Results

In Table 5, we compare CO and Brackett line emission as qualitative indicators of mass loss. Table 6 presents the properties of the sources needed for a quantitative comparison: distances and the resulting Br α luminosity ($F_l^*(\text{Br}\alpha)d^2$) and mass-loss rates derived from CO ($\dot{M}[\text{CO}]$). Table 6 also contains stellar properties such as spectral type, mass, and luminosity (Levreault 1985 and references therein). When the Br α line was not observed, but upper limits on F_l (Br γ) are available, we have estimated an upper limit to the Br α line flux from the upper limit on F_l^* (Br γ) and the average Br α /Br γ ratio of 1.3; this admittedly dubious procedure is not critical to our conclusions. The upper limits on $\dot{M}(\text{CO})$ when no outflow was detected are obtained from Levreault's (1985) estimate of $\dot{M} = 10^{-8} M_\odot \text{ yr}^{-1}$ as his upper limit on undetected lines. This upper limit was estimated for an outflow at a distance of 150 pc. The proper way to scale this upper limit for distance depends on whether or not the source is resolved. We use $\dot{M} = \dot{M}(150 \text{ pc})d/150 \text{ pc}$ which assumes the sources are unresolved and gives the most conservative limit. No upper limits to $\dot{M}(\text{CO})$ are given for XZ Tauri or the C-S star (Cohen and Schwartz 1979) because of possible source confusion (see below).

Table 5 compares Brackett line emission, CO line wings, and radio continuum emission as qualitative indicators of mass loss. Of the 16 objects in Table 5, only five have *both* CO line wings and Brackett emission. Radio continuum emission is detected only for three of the eight stars with CO outflows. This result is different from that of Snell and Bally (1986) who

TABLE 5
QUALITATIVE INDICATIONS OF MASS LOSS

| | Detected CO Flow | |
|-----|--|--|
| | Yes | No |
| | Brackett emission | |
| Yes | Lk H α 198 T Tau* HL Tau* V380 Ori MWC 1080 | DG Tau* XZ Tau* AB Aur Z CMa* R Mon* |
| No | RNO 13 RNO 15 L1551 IRS 5* | RY Tau C-S Star FU Ori |

* We did not detect Br γ emission from R Mon, but Br α was detected from R Mon by Persson *et al.* 1984.

* Indicates the detection of radio continuum emission.

TABLE 6
 PROPERTIES OF SOURCES

| No. | Source | d (pc) | Ref. | $F_{\text{Br}\alpha}^* d^2$ (10^{+21} W) | Sp. Type | Ref. | $\dot{M}(\text{CO})$ ($M_{\odot} \text{ yr}^{-1}$) | L (L_{\odot}) | M (M_{\odot}) |
|---------|--------------------|-------------|------|--|----------|------|---|------------------------|------------------------|
| 1..... | Lk H α 198 | 950 | 1 | 630 ± 100 | B3 | 8 | 3.2×10^{-7} | 950 | 5.0 |
| 2..... | RNO 13 | 350 | 2 | $< 71^a$ | K7: | 7 | 3.4×10^{-7} | 5.2 | 1.0 |
| 3..... | RNO 15 | 350 | 2 | ... | ... | ... | 3.6×10^{-7} | 6.4 | ... |
| 4..... | RY Tau | 140 | 3 | $< 86^a$ | K1 | 8 | $< 10^{-8b}$ | 11.4 | 2.2 |
| 5..... | T Tau | 140 | 3 | 22 ± 2.5 | K1 | 8 | 1.4×10^{-7} | 18.3 | 2.7 |
| 6..... | DG Tau (1983) | 140 | 3 | 11 ± 1.8 (7.8 ± 1.9) | Ge: | 9 | $< 10^{-8b}$ | 7.2 | 1.8 |
| 7..... | L1551 IRS 5 | 140 | 3 | $< 81^a$ | K2 | 10 | 3.9×10^{-7} | 26.3 | 2.7 |
| 8..... | HL Tau (1983) | 140 | 3 | 9.7 ± 2.3 (17 ± 1.8) | K7: | 11 | 4.1×10^{-8c} | 8.5 | 1.0 |
| 9..... | XZ Tau | 140 | 3 | 3.9 ± 1.1 | M3 | 8 | ... ^c | 4.2 | 0.2 |
| 10..... | AB Aur | 140 | 3 | 630 ± 60 | B9e | 12 | $< 10^{-8b}$ | 39.3 | 2.9 |
| 11..... | C-S Star | 480 | 4 | $< 300^a$ | G8 | 13 | ... ^c | 36 | 2.8 |
| 12..... | V380 Ori (1985) | 480 | 4 | 270 ± 30 (250 ± 25) | A1e | 12 | 6.4×10^{-7} | 140 | 3.4 |
| 13..... | FU Ori | 480 | 4 | $< 220^a$ | F2I pec | 8 | $< 3 \times 10^{-8b}$ | 220 | ... |
| 14..... | R Mon | 800 | 5 | $< 370^a$ | B0 | 8 | $< 5 \times 10^{-8b}$ | 1030 | 7.5 |
| 15..... | Z CMa | 1150 | 6 | 4000 ± 700 | B9: | 14 | $< 8 \times 10^{-8b}$ | 6800 | 10.6 |
| 16..... | MWC 1080 | 2200 | 7 | $14,000 \pm 1700$ | B0: | 8 | 3.1×10^{-6} | 6500 | 12.7 |

^a Upper limit to $F_i^*(\text{Br}\alpha)$ from $F_i^*(\text{Br}\gamma)$ and average $F_i^*(\text{Br}\alpha)/F_i^*(\text{Br}\gamma) = 1.3$.

^b Upper limits on $\dot{M}(\text{CO})$ are $10^{-8} M_{\odot} \text{ yr}^{-1} \times (d/150)$ (Levreault 1985, p. 209).

^c Identification of outflow source in question.

REFERENCES FOR DISTANCES AND SPECTRAL TYPES.—(1) Herbig 1960; (2) Herbig and Jones 1983; (3) Elias 1978; (4) Genzel *et al.* 1981; (5) Jones and Herbig 1982; (6) Herbst, Racine, and Warner 1978; (7) Levreault 1985; (8) Cohen and Kuhi 1979; (9) Kuhi 1974; (10) Mundt *et al.* 1985; (11) Cohen 1983; (12) Finkenzeller and Mundt 1984; (13) Cohen and Schwartz 1979; (14) Strom, Grasdalen, and Strom 1974.

found radio emission from most of the (generally more luminous) outflow sources that they observed, with the notable exception of IRC2 in Orion. The assignments to the categories in Table 5 may sometimes be uncertain because of sensitivity limits or questions about which source is driving a molecular outflow (e.g., HL or XZ Tau, Levreault 1985; the C-S star, Pravdo *et al.* 1985), or even the presence of a molecular outflow (R Mon, Levreault 1985). Still, the data are sufficient to conclude that no one of the three indicators is *necessarily* present in stars that are clearly losing mass, and surveys for mass loss activity should not be confined to a single technique.

Both Brackett line emission and CO outflows have been used to estimate mass-loss rates for pre-main-sequence stars. We compare these techniques as quantitative measures of \dot{M} by plotting in Figure 4 the Br α luminosity and the stellar mass-loss rate derived from CO, $\dot{M}(\text{CO})$. The two lines in Figure 4 represent predictions of the Br α luminosity as a function of \dot{M} for the constant velocity and hybrid velocity models of Simon *et al.* (1983), assuming $r_o/r_i \gg 1$. While there does appear to be a correlation between Br α luminosity and $\dot{M}(\text{CO})$, the great majority of sources [all except those with upper limits on $\dot{M}(\text{CO})$] have too little Br α emission. For these stars, the Brackett lines interpreted with the models of Simon *et al.* would give mass-loss rates which are systematically lower than $\dot{M}(\text{CO})$, typically by 1–2 orders of magnitude. The most striking discrepancy is L1551 IRS 5 for which we have plotted the Br α upper limit (No. 7) of Smith *et al.* (1987); it would indicate a mass-loss rate about 3 orders of magnitude lower than that deduced from the CO.

In the following sections, we consider several explanations for this discrepancy: (1) the CO method overestimates \dot{M} ; (2) $\dot{M}(\text{CO})$ gives a correct estimate of the ionized wind strength, but emission from the wind is much lower than in the models

of Simon *et al.* (1983); (3) the stellar wind is primarily neutral; (4) the mass-loss rates are time variable, primarily decreasing with time; and (5) outflowing CO does not represent matter swept up in a stellar wind.

i) Problems with $\dot{M}(\text{CO})$

The fact that the Brackett line emission indicates lower mass-loss rates than does the CO may simply reflect uncertainties in the models used to obtain mass-loss rates (see, e.g., Cabrit and Bertout 1986). Levreault (1985) analyzed the uncertainties in his determinations of $\dot{M}(\text{CO})$; he argues that they are about an order of magnitude, but that $\dot{M}(\text{CO})$ is more likely to underestimate than to overestimate the actual \dot{M} , assuming that the outflows are “momentum conserving” (i.e., that pressure from a hot bubble is not important in accelerating the molecular material). This assumption is well justified on both observational and theoretical grounds for the sources in this study, although it may not be correct for more luminous sources (Kwok and Volk 1985). For the particular case of L1551 IRS 5 a study of far-infrared emission which is extended over the whole molecular outflow (Edwards *et al.* 1986) shows explicitly that the outflow is not “energy-conserving,” because the luminosity of the bipolar infrared emission exceeds the mechanical luminosity of the molecular outflow by more than an order of magnitude. Thus the great majority of the energy in the stellar wind is not translated into kinetic energy of the molecular outflow. Furthermore, the luminosity of the bipolar infrared emission agrees well with that of the stellar wind inferred from $\dot{M}(\text{CO}) = 10^{-6}$ (Snell and Schloerb 1985) and a stellar wind velocity of 300 km s^{-1} (Mundt *et al.* 1985). This fact makes the nondetection of the Brackett lines in this source even more puzzling. Uncertainties in $\dot{M}(\text{CO})$ are unlikely to explain most of the discrepancies in Figure 4.

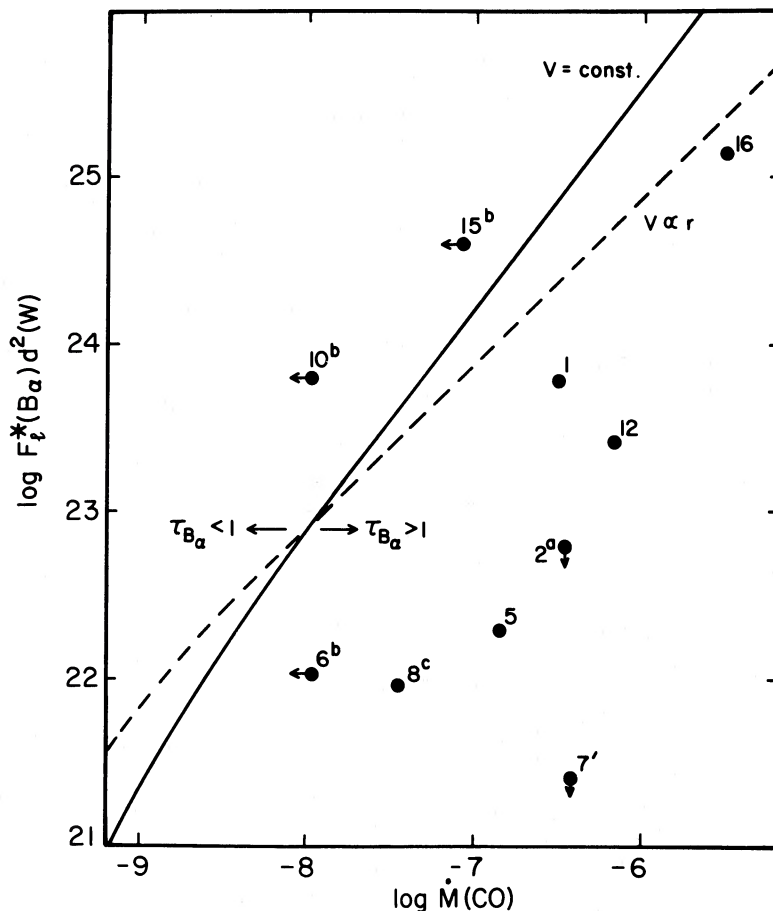


FIG. 4.—The Br α luminosity ($F_l^*(\text{Br}\alpha)d^2$) is plotted vs. the mass-loss rate deduced from CO observations. The Br α flux for L1551 IRS 5 (point 7') is taken from Smith *et al.* (1987). The numbers refer to the source numbers given in the tables. The superscripts on the numbers have the same meaning as in Table 6. The solid line shows the predictions of Simon *et al.* (1983) for constant velocity outflows, and the dashed line shows the predictions for a $v \propto r$ outflow.

ii) Problems with the Stellar Wind Models

The major assumptions in the models of Simon *et al.* (1983) are that the winds are spherically symmetric, that the hydrogen levels are in LTE, and that the winds are fully ionized and isothermal. The lines in Figure 4 are computed for $T = 10^4$ K and $r_o/r_i \gg 1$. If the wind recombines before the Br α emission reaches its asymptotic value, the Br α line flux would decrease for a given mass-loss rate. Based on the Br α /P γ ratios, this effect is unlikely to decrease $F_l^*(\text{Br}\alpha)$ by factors of more than 2–3, not enough to explain most of the discrepancies in Figure 4.

Departures from spherical symmetry are more likely to increase the line flux for a given mass-loss rate (Hamann and Simon 1986). For optically thick emission, the emission for a given amount of material is minimized by minimizing the surface area to volume ratio, which corresponds to a sphere. Thus, nonspherical models make the discrepancy between the infrared lines and the CO still worse.

Departures from LTE in the hydrogen level populations can affect the optical depths and source functions. The non-LTE calculations of Höflich and Wehrse (1987) indicate that the Br α source function may be reduced by factors ~ 10 under some conditions (P. Höflich, private communication). Further study of non-LTE effects is clearly needed to see if they can explain the data in Figure 4.

The predictions in Figure 4 also assume that the winds are isothermal at 10^4 K. Temperature variations in the winds are likely (see, e.g., Höflich and Wehrse 1987). Temperatures above 10^4 K will produce weaker emission lines; at $T = 10^5$ K, the Br α emission can be decreased by factors of 2–6. If, on the other hand, the temperature drops much below 10^4 K, the gas is unlikely to remain fully ionized, leading us to consider winds which are primarily neutral.

iii) Neutral Winds

Predominantly neutral winds could readily explain the discrepancies in Figure 4. Since the Brackett lines in a stellar wind arise quite close to the star, this explanation requires that the wind must be neutral at very small radii; for sources with radio emission, this would be a problem because the radio emission comes from a much larger radius (see the Figs. 1 and 4 of Simon *et al.* 1983). If, however, the radio emission can be attributed to some other mechanism, this constraint could be removed and partially neutral winds could reconcile the CO and infrared line data. In their study of generally more luminous objects, McGregor, Persson, and Cohen (1984) interpreted their detections of the O I line at 8446 Å as implying that the H I lines arise in predominantly neutral regions. Theoretical support for neutral winds comes from recent modeling by Natta, Giovanardi, and Palla (1987) of winds from low-mass,

cool stars of the type we are studying. They find that when the electron temperature drops below 7000 K, the ionized fraction drops sharply ($X_e < 0.1$), and the infrared line emission is 10–100 times less than that from fully ionized winds.

iv) *Decreasing Mass-Loss Rates*

One of the more interesting explanations for weak infrared lines is a decrease in the mass-loss rate with time. The CO-derived mass-loss rate averages over the lifetime of the outflow (typically 10^4 – 10^5 yr in these objects) while the infrared lines average over a much shorter time (the crossing time for the region of Br α emission is less than 10^3 s). Before this feature can be exploited to constrain the evolution of mass loss in pre-main-sequence stars, the alternative explanations discussed above would have to be ruled out. Finally, the bipolar infrared emission in L1551 (Edwards *et al.* 1986) argues against this explanation because the cooling time of the dust is short enough that the full energy inferred for the stellar wind must have been deposited fairly recently. In that source, there is evidence for an ongoing stellar wind. L1551 provides the strongest evidence for a partly (or largely) neutral wind, but in this interpretation, the radio continuum emission must also have a different origin, such as shock-ionized gas (see § IVc).

v) *Alternative Explanations for Molecular Outflows*

The basic model used to derive mass-loss rates from CO assumes that the molecular outflow is ambient molecular cloud material swept up by a much faster stellar wind. If this basic picture is wrong, the derived mass-loss rates will be incorrect. Pudritz and Norman (1983, 1986) and Uchida and Shibata (1985) have proposed that molecular outflows originate in the outer part of a rotating magnetized disk, while an ionized wind may be driven from the inner part (Pudritz 1985). In this picture, the connection between the molecular outflow and the faster, ionized wind is less direct. In the particular case discussed by Pudritz and Norman (1986), the ratio of the ionized and molecular mass-loss rates is a strong function of the disk mass and would be expected to increase as the system evolves and the disk mass decreases. However, ionized winds may also arise from the star itself at later stages. In general this class of models could explain the poor correlation of Brackett emission and molecular outflows, but they are not sufficiently defined to make specific predictions for comparison to our observations.

c) *Other Aspects of the Data*

We recall that none of the infrared lines shows clear evidence of being spectrally resolved, with limits of less than 200 km s^{-1} for the lines with good signal-to-noise ratio. A higher resolution study of Br α lines in (mostly) more luminous objects (Persson *et al.* 1984) also found many line widths to be less than 200 km s^{-1} . Many of the objects in our sample have H α emission lines with widths $\gtrsim 300 \text{ km s}^{-1}$. For AB Aurigae, a recent study of Mg II lines gives terminal velocities of 370–495 km s^{-1} (Praderie *et al.* 1986). Because the infrared lines have lower optical depths than does H α , they will arise closer to the stellar surface. Then the smaller line widths would suggest that the expansion velocity increases with distance from the star. This interpretation, suggested by the interpretation of the Be

star γ Cas by Chalabaev and Maillard (1985), can be pursued with higher resolution infrared spectroscopy, combined with simultaneous optical spectroscopy. Such observations can also test suggestions that the winds are collimated (see model profiles in Hamann and Simon 1986).

The H $_2$ emission in T Tau, and probably, in L1551 IRS 5 and MWC 1080, indicates the presence of shocked molecular material near the star. This fact supports the idea that the stellar wind does not simply expand freely into a cavity but is resisted in some directions by, for example, a neutral disk. The radio emission from L1551 IRS 5 includes two compact sources which Bieging and Cohen (1985) have interpreted as a binary system. However, unlike the case of T Tauri, the radio emission from the two components is nearly equal; and Rodriguez *et al.* (1986) have interpreted the two sources as shock-ionized gas from a neutral wind as it strikes the inner edges of a disk, rather than as two separate stars. The molecular hydrogen emission could then arise in the shocked matter in the disk.

V. SUMMARY

1. Brackett line emission was detected from nine of 16 pre-main-sequence stars. Molecular hydrogen emission was confirmed in T Tauri and marginally detected in L1551 IRS 5 and MWC 1080. Radio continuum emission was detected from four of these objects. The line fluxes appear to vary on time scales of years but not of days.

2. Comparison of the Br α , Br γ , Pf γ , and radio continuum emission clearly indicates that the emission does not come from optically thin H II regions. Simple models of optically thick emission from stellar winds provide a better match to our data, but they also have some problems. The fact that the radio continuum emission is extended argues that it is not produced in a spherical stellar wind. We conclude that for these stars, radio emission is a poor measure of the ionized mass-loss rate. There are also problems with the infrared lines, but they are less severe.

3. Comparison of these indicators of ionized mass loss with the mass loss inferred from CO data reveals the same problem often seen in higher mass objects. The mass-loss rates inferred from the CO data and momentum conservation, when combined with the models of Simon *et al.* (1983) for the ionized wind, predict much stronger infrared line and radio continuum emission than we see. We have considered a number of possible reasons for this problem. While the interpretation of both the CO and infrared/radio data are subject to question, most effects will aggravate the problem. Three other explanations, largely neutral winds, a decreasing mass-loss rate, and disk-driven models for outflows have also been considered. The most attractive explanation is that the winds are largely neutral, but the other possibilities cannot be ruled out at the present time.

We would like to thank the staffs of the IRTF and the VLA for their assistance during these observations. This work was supported in part by NSF grant AST 83-12332 to The University of Texas at Austin and AST 84-03054 to Cornell University and by the Sloan Foundation.

REFERENCES

- Appenzeller, I., Jankovics, I., and Ostreicher, R. 1984, *Astr. Ap.*, **141**, 108.
 Bally, J., and Lada, C. J. 1983, *Ap. J.*, **265**, 824.
 Becker, R. H., and White, R. L. 1985, *Ap. J.*, **297**, 649.
 Becklin, E. E., Matthews, K., Neugebauer, G., Willner, S. P. 1978, *Ap. J.*, **220**, 831.
 Beckwith, S., Evans, N. J., II, Gatley, I., Gull, G., and Russell, R. W. 1983, *Ap. J.*, **264**, 152.
 Beckwith, S., Gatley, I., Matthews, K., and Neugebauer, G. 1978, *Ap. J. (Letters)*, **223**, L41.
 Bertout, C. 1984, *Ap. J.*, **285**, 269.

- Biegging, J. H., and Cohen, M. 1985, *Ap. J. (Letters)*, **289**, L5.
 Biegging, J. H., Cohen, M., and Schwartz, P. R. 1984, *Ap. J.*, **282**, 699.
 Brown, A., Drake, S. A., and Mundt, R. 1986, preprint.
 Brown, A., Jordan, C., Millar, T. J., Godhalekar, P., and Wilson, R. 1981, *Nature*, **290**, 34.
 Brown, A., Mundt, R., and Drake, S. A. 1985, in *Radio Stars*, ed. R. M. Hjellming and D. M. Gibson (Dordrecht: Reidel), p. 105.
 Cabrit, S., and Bertout, C. 1986, *Ap. J.*, **307**, 313.
 Campins, H., Rieke, G. H., and Lebofsky, M. J. 1985, *A.J.*, **90**, 896.
 Chalabaev, A. A. 1986, in Proc. 9th European Astronomical Meeting, in preparation.
 Chalabaev, A. A., and Maillard, J. P. 1985, *Ap. J.*, **294**, 640.
 Cohen, M. 1983, *Ap. J. (Letters)*, **270**, L69.
 Cohen, M., Biegging, J. H., and Schwartz, P. R. 1982, *Ap. J.*, **253**, 707.
 Cohen, M., and Kuhl, L. V. 1979, *Ap. J. Suppl.*, **41**, 743.
 Cohen, M., and Schwartz, R. D. 1979, *Ap. J. (Letters)*, **233**, L77.
 Draine, B. T. 1983, *Ap. J.*, **270**, 519.
 Edwards, S., Strom, S. E., Snell, R. L., Jarrett, T. H., Beichman, C. A., and Strom, K. M. 1986, *Ap. J. (Letters)*, **307**, L65.
 Elias, J. H. 1978, *Ap. J.*, **224**, 857.
 Feigelson, E. D., and Montmerle, T. 1985, *Ap. J. (Letters)*, **289**, L19.
 Felli, M., Gahm, G. F., Harten, R. H., Liseau, R., and Panagia, N. 1982, *Astr. Ap.*, **107**, 354.
 Finkenzeller, U., and Mundt, R. 1984, *Astr. Ap. Suppl.*, **55**, 109.
 Genzel, R., Reid, M. J., Moran, J. M., and Downes, D. 1981, *Ap. J.*, **244**, 884.
 Hamann, F., and Simon, M. 1986, *Ap. J.*, **311**, 909.
 Hartmann, L., Edwards, S., and Avrett, E. 1982, *Ap. J.*, **261**, 279.
 Herbig, G. H. 1960, *Ap. J. Suppl.*, **4**, 337.
 Herbig, G. H., and Jones, B. F. 1983, *A.J.*, **88**, 1040.
 Herbig, G. H., Racine, R., and Warner, J. W. 1978, *Ap. J.*, **223**, 471.
 Herbst, W., Racine, R., and Warner, J. W. 1978, *Ap. J.*, **223**, 471.
 Höflich, P., and Wehrse, R. 1987, *Astr. Ap.*, in press.
 Jones, B. F., and Herbig, G. H. 1982, *A.J.*, **87**, 1223.
 Königl, A. 1982, *Ap. J.*, **261**, 115.
 Kuhl, L. V. 1964, *Ap. J.*, **140**, 1409.
 ———. 1974, *Astr. Ap. Suppl.*, **15**, 47.
 Kwok, S., and Volk, K. 1985, *Ap. J.*, **299**, 191.
 Lada, C. J. 1985, *Ann. Rev. Astr. Ap.*, **23**, 267.
 Levreault, R. M. 1985, Ph.D. thesis, The University of Texas at Austin.
 Landini, M., Natta, A., Oliva, E., Salinari, P., Moorwood, A. F. M. 1984, *Astr. Ap.*, **134**, 284.
 McGregor, P. J., Persson, S. E., and Cohen, J. G. 1984, *Ap. J.*, **286**, 609.
 Mundt, R., Stocke, J., Strom, S. E., Strom, K. M., and Anderson, E. R. 1985, *Ap. J. (Letters)*, **297**, L41.
 Natta, A., Giovanardi, C., and Palla, F. 1987, in preparation.
 Panagia, N., and Felli, M. 1975, *Astr. Ap.*, **39**, 1.
 Persson, S. E., Geballe, T. R., McGregor, P. J., Edwards, S., and Lonsdale, C. J. 1984, *Ap. J.*, **286**, 289.
 Phillips, T. G., and Beckman, J. 1980, *M.N.R.A.S.*, **193**, 245.
 Praderie, F., Simon, T., Catala, C., and Boesgaard, A. M. 1986, *Ap. J.*, **303**, 311.
 Pravdo, S. H., Rodriguez, L. F., Curiel, S., Canto, J., Torrelles, J. M., Becker, R. H., and Sellgren, K. 1985, *Ap. J. (Letters)*, **293**, L35.
 Pudritz, R. 1985, *Ap. J.*, **293**, 216.
 Pudritz, R. E., and Norman, C. A. 1983, *Ap. J.*, **274**, 677.
 ———. 1986, *Ap. J.*, **301**, 571.
 Reynolds, S. P. 1986, *Ap. J.*, **304**, 713.
 Rieke, G. H., and Lebofsky, M. J. 1985, *Ap. J.*, **288**, 618.
 Rodriguez, L. F., Canto, J., Torrelles, J. M., and Ho, P. T. P. 1986, *Ap. J. (Letters)*, **301**, L25.
 Schmid-Burgk, J. 1982, *Astr. Ap.*, **108**, 169.
 Schwartz, P. R., Simon, T., and Campbell, R. 1986, *Ap. J.*, **303**, 233.
 Simon, M., Felli, M., Cassar, L., Fischer, J., and Massi, M. 1983, *Ap. J.*, **266**, 623.
 Smith, H. A., Fischer, J., Geballe, T. R., and Schwartz, P. R. 1987, *Ap. J.*, **316**, 265.
 Snell, R. L., and Bally, J. 1986, *Ap. J.*, **303**, 683.
 Snell, R. L., Bally, J., Strom, S. E., and Strom, K. M. 1985, *Ap. J.*, **290**, 587.
 Snell, R. L., and Schloerb, P. 1985, *Ap. J.*, **295**, 490.
 Spitzer, L. 1978, *Physical Processes in the Interstellar Medium* (New York: Wiley), p. 29.
 Strom, S. E., Grasdalen, G. L., and Strom, K. M. 1974, *Ap. J.*, **191**, 111.
 Thompson, R. I. 1987, *Ap. J.*, **312**, 784.
 Torbett, M. V. 1984, *Ap. J.*, **278**, 318.
 Uchida, Y., and Shibata, K. 1985, *Pub. Astr. Soc. Japan*, **37**, 515.
 Zinnecker, H., Mundt, R., Williams, P. M., and Zealey, W. J. 1985, *Mitt. Astr. Ges.*, **63**, 234.

STEVE BECKWITH and MIKE SKRUTSKIE: Department of Astronomy, Space Science Building, Cornell University, Ithaca, NY 14853

NEAL J. EVANS II: Department of Astronomy, The University of Texas at Austin, Austin, TX 78712-1083

RUSSELL M. LEVREULT: Center for Astrophysics, 60 Garden Street, Cambridge, MA 02138